HHS Public Access

Author manuscript

Dev Biol. Author manuscript; available in PMC 2016 April 29.

Published in final edited form as:

Dev Biol. 2015 March 15; 399(2): 218–225. doi:10.1016/j.ydbio.2014.12.032.

Diverse ETS transcription factors mediate FGF signaling in the *Ciona* anterior neural plate

T. Blair Gainous[1], **Eileen Wagner**, and **Michael Levine**[*]

Center for Integrative Genomics, Division of Genetics, Genomics and Development, Department of Molecular and Cell Biology, University of California, Berkeley, CA 94720, USA

Abstract

The ascidian *Ciona intestinalis* is a marine invertebrate belonging to the sister group of the vertebrates, the tunicates. Its compact genome and simple, experimentally tractable embryos make *Ciona* well-suited for the study of cell-fate specification in chordates. Tunicate larvae possess a characteristic chordate body plan, and many developmental pathways are conserved between tunicates and vertebrates. Previous studies have shown that FGF signals are essential for neural induction and patterning at sequential steps of *Ciona* embryogenesis. Here we show that two different ETS family transcription factors, Ets1/2 and Elk1/3/4, have partially redundant activities in the anterior neural plate of gastrulating embryos. Whereas Ets1/2 promotes pigment cell formation in lateral lineages, both Ets1/2 and Elk1/3/4 are involved in the activation of *Myt1L* in medial lineages and the restriction of *Six3/6* expression to the anterior-most regions of the neural tube. We also provide evidence that photoreceptor cells arise from posterior regions of the presumptive sensory vesicle, and do not depend on FGF signaling. Cells previously identified as photoreceptor progenitors instead form ependymal cells and neurons of the larval brain. Our results extend recent findings on FGF-dependent patterning of anterior–posterior compartments in the *Ciona* central nervous system.

Keywords

Ciona intestinalis; FGF; ETS; Neural patterning

Introduction

The *Ciona* larval central nervous system (CNS) consists of fewer than 400 cells and can be divided into three territories, corresponding to the forebrain/midbrain, hindbrain, and spinal cord of vertebrates (Nicol and Meinertzhagen, 1991; Wada et al., 1998; Imai et al., 2009). The sensory vesicle (simple brain), encompassing the forebrain/midbrain region, contains pigmented cells of the otolith and ocellus, as well as associated photoreceptors. The motor ganglion corresponds to the hindbrain region of vertebrates, and the caudal neural tube extends the length of the tail. The *Ciona* neural plate, as classically defined, also gives rise to a region of neurogenic ectoderm located anterior to the neural tube. This territory forms

[*]Corresponding author. mlevine@berkeley.edu (M. Levine).

[1]Present address: Cardiovascular Research Institute, University of California, San Francisco, CA 94158-2517, USA.

placode-like derivatives, including the adhesive palps at the rostral end of the tadpole larva (Veeman et al., 2010; Wagner and Levine, 2012), the oral siphon placode, and epidermal sensory neurons.

Fibroblast growth factor (FGF) signaling has been implicated in induction and subsequent patterning of the vertebrate CNS (Altmann and Brivanlou, 2001). However, the complex interplay of multiple developmental cues in the context of thousands of cells can make the precise roles of signaling and transcriptional pathways difficult to investigate in vertebrate embryos. FGF signaling is also essential for neural induction and patterning in *Ciona*. Anterior (a-line) neural tissue in *Ciona* is induced in the bilateral a6.5 blastomeres of the 32-cell embryo by FGF signaling from neighboring vegetal blastomeres (Hudson and Lemaire, 2001; Lemaire et al., 2002). FGF induces expression of a number of target genes, including *Otx*, via ETS and GATA transcription factors (Bertrand et al., 2003; Rothbächer et al., 2007; Khoueiry et al., 2010). Following one round of cell division, at the 64-cell stage, *Dmrt* is expressed in the daughters of a6.5 (a7.9 and a7.10) and in the neighboring a7.13 cells, all of which maintain contact with the vegetal source of FGF. *Dmrt* expression is dependent on FGF and FoxA, and is required for formation of anterior neural structures. The six $Dmrt^{+}$ cells are the precursors to the entire anterior neural plate, eventually giving rise to both anterior sensory vesicle and the placode-like territory (Imai et al., 2006, Tresser et al., 2010; Wagner and Levine, 2012). It has recently been shown that FGF signaling is required again between the 64- and 112-cell stages to establish the boundary between the anterior and posterior daughters of the $Dmrt^{+}$ lineage, which defines the anterior limits of the neural tube. The posterior daughters (a8.19, a8.17, and a8.25) receive an FGF signal, leading to repression of *FoxC* and expression of *ZicL*. The $ZicL^{+}$ cells contribute to the anterior neural tube, whereas the anterior daughters (a8.20 and a8.18) express *FoxC* and contribute to the palps and peripheral nervous system (Wagner and Levine, 2012; summarized in Supplementary Fig. 1).

The 112-cell stage is followed by the onset of gastrulation and another A–P oriented cell division in the nascent neural plate. At the mid-gastrula stage, the neural plate is composed of a 6-row grid of cells, denoted from posterior to anterior as rows I–VI (Fig. 1A). Rows I–IV contribute to the definitive neural tube, whereas rows V and VI form the adhesive palps, oral siphon placode, and rostral trunk epidermal neurons (RTENs; Fig. 1B). At this stage, FGF expression is restricted to row II, and the MAP kinase (MAPK) pathway component ERK1/2 is activated in the neighboring rows I and III (Hudson et al., 2007; Haupaix et al., 2014). Several recent studies show that FGF signaling is required for the specification of the pigmented cells of the otolith and ocellus, which arise from the lateral a9.49 cells of row III (Squarzoni et al., 2011; Haupaix et al., 2014; Racioppi et al., 2014).

Here, we present evidence that FGF signaling is also important for the specification of medial lineages of row III. Using both pharmacological and genetic perturbations, we show that inhibition of FGF signaling beginning at the 112-cell stage transforms both lateral and medial cells of row III to a row IV-like fate. We also show that two different ETS family transcription factors mediate FGF signaling in row III. Whereas previous studies have shown that Ets1/2 is required in the lateral pigment cell precursors (PCPs; Squarzoni et al., 2011; Abitua et al., 2012; Racioppi et al., 2014), an additional ETS family transcription factor,

Elk1/3/4, also appears to play a role in specifying row III cells. Dominant negative forms of Ets1/2 and Elk1/3/4 cause ectopic expression of *Six3/6* (a row IV marker gene) in row III, loss of expression of the medial row III marker *Myt1L*, and loss of pigmented cells. A constitutive activator form of Elk1/3/4 has reciprocal effects on *Six3/6* and *Myt1L* expression patterns. However, in contrast to an Ets1/2 constitutive activator, the Elk1/3/4 activator does not produce supernumerary pigmented cells. We also provide evidence that the photoreceptor cells of the *Ciona* larva do not derive from medial row III as previously reported (Cole and Meinertzhagen, 2004; Horie et al., 2005; Russo et al., 2014), but instead arise from a more posterior region of the neural plate (i.e., row II).

Materials and methods

Animals and electroporations

Adult *Ciona intestinalis* were obtained from M-REP (San Diego, CA, USA) and maintained in artificial sea water (ASW) at 18 °C under constant illumination. Gamete isolation, fertilization, and electroporations were performed as described (Christiaen et al., 2009a,b). 15–60 μg of each reporter or perturbation plasmid was used in electroporations, with combined plasmids not exceeding 200 μg total. Each experiment was repeated at least twice. For drug treatments, embryos were transferred to ASW containing 0.1% DMSO or 10 μM U0126 (Promega) in DMSO. For fluorescence microscopy, embryos and larvae were fixed in MEM-FA (3.7% formaldehyde, 0.1 M MOPS pH7.4, 0.5 M NaCl, 1 mM EGTA, 2 mM $MgSO_4$, 0.05% Triton X-100) for 20 min at room temperature, and then washed several times in PBTT (PBS+50 mM NH_4Cl+0.3% Triton X-100) and PBTr (PBS+0.01% Triton X-100). For Phalloidin staining, embryos or larvae were incubated overnight at 4 °C with Alexa Fluor 647-conjugated Phalloidin (Molecular Probes; 1:500) in PBS+0.01% Tween-20, and then rinsed with PBS+0.005% Triton X-100. Samples were mounted in 50% glycerol in PBS with 2% DABCO. Imaging was performed on a Zeiss Axio Imager.A2 upright fluorescence microscope or a Zeiss LSM 700 laser scanning confocal microscope. Reporter colocalization was determined using Volocity imaging software (PerkinElmer). Larvae showing expression of the *Arrestin* reporter were chosen at random and imaged by confocal microscopy. Confocal stacks were imported into Volocity, and for each image a region of interest was drawn around the trunk of the larva and thresholded Pearson's correlation coefficient was determined.

Molecular cloning

Dmrt, ZicL, Six3/6, and *Arrestin* regulatory sequences have been reported previously (Wagner and Levine, 2012; Shi and Levine, 2008; Christiaen et al., 2007; Yoshida et al., 2004). *Tyrp1a* regulatory sequence was obtained from DBTGR (http://dbtgr.hgc.jp), amplified with AscI-*Tyrp1a* -1700 F (5′-ATGGCGCGCCGCCTGGGTTTCTATGTTCATC; underlining indicates restriction site used for cloning) and NotI-*Tyrp1a* +7 R (5′-ATGCGGCCGCTGTAGAATAAGTACAGATCTTTCAAC), and cloned into a *LacZ*-containing expression vector. *dnFGFR* was digested from *Dmrt > dnFGFR* (Wagner and Levine, 2012) using NotI and BlpI and cloned downstream of the *ZicL* enhancer. Coding sequence for the N-terminal 224 amino acids of Elk1/3/4 (containing the ETS DNA-binding domain) was amplified from *Dmrt > Elk* (Wagner and Levine, 2012) using NheI-*Elk* CDS F

(5′-ATGCTAGCAATGATGACATTGAAAATCGACACAG) and NgoMIV-*Elk* DBD R (5′-TATGCCGGCCCCTTCGTCGTCATCATC). Three-way ligation was performed to clone this fragment and an NgoMIV/BlpI-digested WRPW fragment into a modified *ZicL* plasmid containing an N-terminal nuclear localization signal (NLS). VP64 was amplified from pTALETF_v2(NN) (Sanjana et al., 2012; Addgene plasmid 32185) using NgoMIV-VP64 F (5′-ATGCCGGCAGCGACGCATTGGACGATTTTG) and BlpI/EcoRI-VP64 R (5′-ATGCTCAGCGAATTCTTACAGCATGTCCAGGTC), and used to replace the WRPW fragment.

Whole mount in situ hybridization and immunohistochemistry

The following clones were obtained from the *C. intestinalis* gene collection release 1: *Six3/6* (GC11m13), *Tyrp1a* (GC44b23) *Ets1/2* (GC21c21), and *Elk1/3/4* (GC27g08). *Myt1L* probe template was obtained by amplifying a segment of *C. intestinalis* genomic DNA corresponding to exon 10 of the *Myt1L* gene model (KH.C1.274.v1.A. SL1-1) using primers NotI-*Myt1L* exon 10 probe F (5′-ATGCGGCCGCGCAAGTGGCCGTCGCAATTC) and EcoRI-*Myt1L* exon 10 probe R (5′-ATGAATTCGCGGAATGGTGCTGACGTTG). This fragment was cloned into the NotI/EcoRI sites of pBSKM, the plasmid backbone used in the gene collection. Templates for probe transcription were made by performing PCR on these plasmids using M13(-20)F (5′-GTAAAACGACGGCCAGT) and M13(-24)R (5′-AGCGGATAACAATTTCACACAGGA), followed by DpnI digestion for 1 h at 37 °C to remove plasmid template. Probes were transcribed using T7 RNA polymerase (NEB) and DIG or Fluorescein RNA labelingmix (Roche). In situ hybridization with immunohistochemistry was performed essentially as described (Christiaen et al., 2009c): Embryos were fixed 2 h at room temperature or overnight at 4 °C in 4% formaldehyde made fresh from paraformaldehyde with 0.1 M MOPS pH7.4, 0.5 M NaCl, 1 mM EGTA, 2 mM $MgSO_4$, and 0.1% Tween-20. After fixation, embryos were rinsed with ice-cold PBS, dehydrated by gradual replacement of PBS with ethanol, and stored in 75% ethanol at −20 °C. Prior to rehydration, embryos were treated with 2% H_2O_2 in methanol for 30 min to quench endogenous peroxidase activity. Samples were then rehydrated and treated with 5 μg/ml Proteinase K in PBT for 15 min at room temperature, post-fixed for 30 min in 4% formaldehyde in PBS, and incubated with DIG and/or Fluorescein-labeled probes overnight at 55 °C. Hybridized embryos were washed as described, equilibrated in TNT (0.1 M Tris pH7.5, 150 mM NaCl, 0.1% Tween-20), blocked in TNB-TSA (0.1 M Tris pH7.5, 150 mM NaCl, 1% Roche blocking reagent), and incubated with anti-DIG-POD (Roche) plus mouse anti-β-galactosidase (Promega; 1:2000) and/or rabbit anti-GFP (Molecular Probes; 1:1000) in TNB-TSA overnight at 4 °C. After extensive TNT washes, signal amplification was performed with a 1:100 dilution of Cy3-conjugated TSA Plus reagent (PerkinElmer) 10–30 min at room temperature followed by several TNT washes and blocking in TNBS (1% Roche Western blocking reagent in TNT plus 2% normal donkey serum). Secondary antibodies (Alexa Fluor 647 Donkey anti-Mouse IgG, Alexa Fluor 488 Donkey anti-Rabbit IgG, or Alexa Fluor 647 Donkey anti-Rabbit IgG; Molecular Probes) were added at 1:500 in TNBS overnight at 4 °C. Samples were washed several times with TNT before mounting in 50% glycerol/PBS+2% DABCO. For double in situ hybridization, anti-DIG-POD activity was quenched with 0.01 N HCl for 10 min following the TSA reaction, followed by TNT washes, blocking with TNB-TSA, and incubation with anti-Fluorescein-POD (Roche). The

following day, a second TSA reaction was performed using Fluorescein-conjugated TSA Plus reagent (PerkinElmer) before proceeding to TNT washes, blocking, and secondary antibody incubation.

Results

FGF signaling is required to pattern the presumptive anterior sensory vesicle

Rows III and IV of the mid-gastrula neural plate contribute to the anterior sensory vesicle (Fig. 1C and D), including the a9.49-derived pigmented cells. It has recently been shown that the a9.49 cells undergo two additional rounds of cell division before becoming post-mitotic, with pigmented cell fates segregating to the posterior granddaughters of a9.49 (Haupaix et al., 2014; Racioppi et al., 2014). While these studies and others have shown that specification of the pigmented cells depends on sequential FGF signaling from mid-gastrula through neurula stages (Squarzoni et al., 2011; Haupaix et al., 2014; Racioppi et al., 2014), the role of FGF in patterning the medial cells of row III (a9.33 and a9.37 pairs) has not been thoroughly investigated.

To determine the role of FGF signaling in patterning medial row III, we performed pharmacological and genetic perturbations and assayed for expression of key patterning markers by in situ hybridization. *Six3/6* is the *Ciona* ortholog of *Six3*, a homeodomain transcription factor expressed in anterior neural tissue throughout the Bilateria (Steinmetz et al., 2010). In *Ciona* embryos, *Six3/6* is specifically expressed in row IV of the 6-row neural plate (Fig. 2A). These cells contribute to the anterior-most regions of the sensory vesicle, with at least some descendants forming neurons of the adult nervous system (T.B.G., unpublished observations). *Myt1L* is a zinc finger transcription factor orthologous to vertebrate MYT1, a neural-specific transcription factor involved in proliferation, differentiation, and production of myelin in oligodendrocyte precursors (Kim and Hudson, 1992; Armstrong et al., 1995; Kim et al., 1997; Nielsen et al., 2004). *Myt1L* is specifically expressed in the medial a9.33 and a9.37 cells of row III during gastrulation (Fig. 2B). The a9.49 pigment cell precursors (PCPs) in lateral row III express a number of genes involved in melanin biosynthesis, including members of the tyrosinase superfamily such as *Tyrp1a* and *Tyr* (Squarzoni et al., 2011; Abitua et al., 2012; Racioppi et al., 2014). Transcripts of *Tyrp1a* can be detected at mid-gastrula stage specifically in the a9.49 PCPs (Fig. 2B).

Ciona embryos were electroporated with a *Dmrt > LacZ* reporter gene and treated with either DMSO or the MEK inhibitor U0126 at the 112-cell stage (4.5 hpf @ 18 °C). Embryos were fixed at mid-gastrula stage (6 hpf @ 18 °C) and processed for in situ hybridization and β-galactosidase (β-gal) immunohistochemistry. Following treatment with U0126 at the 112-cell stage, the anterior neural boundary is maintained, as evidenced by normal expression of a *ZicL* reporter (Supplementary Fig. 2). However, *Six3/6* expression expands posteriorly into row III, whereas expression of *Tyrp1a* and *Myt1L* in lateral and medial regions of row III, respectively, is abolished (Fig. 2C and D).

FGF signals are transduced by MEK via the MAPK pathway. To determine whether MEK-dependent patterning of the mid-gastrula neural plate is indeed mediated by FGF, we expressed a dominant-negative form of the FGF receptor (*dnFGFR*) using the *ZicL*

enhancer, which mediates expression throughout the presumptive neural tube. The *ZicL > dnFGFR* transgene recapitulates the patterns of gene expression obtained with U0126 treatment, including expansion of *Six3/6* expression (compare Fig. 2E and E′ with G and G′; Supplementary Fig. 5) and loss of *Myt1L* and *Tyrp1a* expression in row III (compare Fig. 2F and F′ with H and H′; Supplementary Fig. 5). These results show that FGF/MEK signaling is important for patterning both medial and lateral cells of row III.

Six3/6 repression is mediated by two ETS family transcription factors

We next sought to identify the effector(s) of FGF signaling involved in repression of *Six3/6* in row III. ETS family transcription factors are common effectors of FGF/MAPK signaling (Sharrocks et al., 1997; Sharrocks, 2001; Oikawa and Yamada, 2003), so we focused our efforts on two ETS family genes expressed in the neural plate of gastrula-stage embryos, *Ets1/2* and *Elk1/3/4* (Squarzoni et al., 2011; Wagner and Levine, 2012; Supplementary Fig. 3). Based on their expression patterns, we hypothesized that *Six3/6* repression in row III may occur downstream of one or both of these factors. We first tested *Ets1/2* since it is a well-characterized effector of FGF signaling in the notochord, brain, and mesenchyme of the ascidian *Halocynthia roretzi* (Miya and Nishida, 2003), as well as heart precursors and pigmented cells in *Ciona* (Davidson et al., 2006; Squarzoni et al., 2011; Abitua et al., 2012; Racioppi et al., 2014).

To test the role of Ets1/2 in the patterning of the anterior neural plate, we took advantage of previously published chimeric repressor and activator fusions of the Ets1/2 DNA-binding domain driven by the *ZicL* enhancer (*ZicL > Ets^{DBD}:WRPW* and *ZicL > Ets^{DBD}:VP16*; Abitua et al., 2012). These fusion proteins are sufficient to abolish pigmentation or induce supernumerary pigmented cells, respectively, when expressed specifically in the a9.49 pigmented cell lineage (Squarzoni et al., 2011) or more broadly with the *ZicL* enhancer (Abitua et al., 2012). However, the effects of these perturbations on patterning of the mid-gastrula neural plate have not been investigated. Embryos were electroporated with *ZicL > Ets^{DBD}:WRPW* or *ZicL > Ets^{DBD}:VP16* and assayed for expression of *Six3/6* and *Myt1L* at mid-gastrula stage by in situ hybridization. Surprisingly, these perturbations had only modest effects on expression of *Six3/6* and *Myt1L* (Fig. 3A–D′; Supplementary Fig. 5). These results, along with previous observations, suggest that while Ets1/2 activity is essential for the specification of pigmented cell fates in the lateral a9.49 lineage, it does not appear to be the sole mediator of FGF-dependent repression of *Six3/6* in row III. We therefore went on to test whether Elk1/3/4 might also play a role in this repression.

Repressor and activator forms of Elk1/3/4 were constructed by fusing coding sequences for an N-terminal 224-amino acid peptide containing the ETS DNA-binding domain to a WRPW repressor motif (*Elk^{DBD}:WRPW*) or VP64 activation domain (*Elk^{DBD}:VP64*). This fragment shows ~65% identity with Ets1/2 within the 67 amino acid residues comprising the minimal DNA binding domain, but exhibits very little conservation outside of this domain (Supplementary Fig. 4). *Elk^{DBD}:WRPW* and *Elk^{DBD}:VP64* fusions were placed downstream of the *ZicL* enhancer and embryos were electroporated with the *ZicL > Elk^{DBD}:WRPW* or *ZicL > Elk^{DBD}:VP64* fusion genes, grown to mid-gastrula stage, and assayed for expression of *Six3/6* and *Myt1L*. The Elk1/3/4 fusion genes have slightly stronger effects on expression

of *Myt1L* and *Six3/6* in rows III and IV than the corresponding Ets1/2 fusions. The majority of embryos electroporated with *ZicL* > *Elk*^{DBD}*:WRPW* exhibit an expansion of the *Six3/6* expression pattern into row III (Fig. 3E and E′). Expansion of *Six3/6* expression is accompanied by the loss of *Myt1L* expression in row III (Fig. 3F and F′). Electroporation of *ZicL* > *Elk*^{DBD}*:VP64* results in a reciprocal phenotype, namely, the loss of *Six3/6* expression in row IV (Fig. 3G and G′), and a corresponding anterior expansion of *Myt1L* expression (Fig. 3H and H′).

Elk1/3/4 and Ets1/2 fusion genes cause distinct larval phenotypes

The preceding results suggest that Ets1/2 and Elk1/3/4 have partially redundant patterning activities in row III of the *Ciona* neural plate. Previous studies have shown that Ets1/2 activity is required for specification of the lateral a9.49 pigmented cell lineage, but the role of Elk1/3/4 has been heretofore unexplored. To further characterize the role of Elk1/3/4 in patterning the anterior neural plate, we examined larvae derived from embryos electroporated with *ZicL* > *dnFGFR*, *ZicL* > *Elk*^{DBD}*:VP64* and *ZicL* > *Elk*^{DBD}*:WRPW*. Whereas control larvae normally have two pigmented cells, *ZicL* > *dnFGFR* larvae lack pigmentation (Fig. 4A and B). The majority of *ZicL* > *Elk*^{DBD}*:VP64* larvae have 1–2 pigmented cells, similar to controls (Fig. 4C). By contrast, the comparable activator form of Ets1/2 results in supernumerary pigmented cells (Fig. 4E; Squarzoni et al., 2011; Abitua et al., 2012). These supernumerary pigmented cells are likely derived from the 8 descendants of a9.49 (4 on each side), rather than from more anterior parts of the neural plate (e.g. a9.50). *ZicL* > *Elk*^{DBD}*:WRPW* results in loss of pigmented cells, similar to *ZicL* > *dnFGFR* and the repressor form of Ets1/2 (Fig. 4D and F; Squarzoni et al., 2011; Abitua et al., 2012).

The distinct pigment cell phenotypes obtained with the Ets1/2 and Elk1/3/4 constitutive activators suggest that Ets1/2 plays an instructive role in pigmented cell formation, whereas Elk1/3/4 is permissive for pigmented cell fates owing to its role in repression of *Six3/6*. In order to test whether ectopic *Six3/6* expression is directly responsible for the loss of pigment cells in *ZicL* > *Elk*^{DBD}*:WRPW* larvae, we misexpressed *Six3/6* in the a9.49 lineage using a *Tyrp1a* > *Six3/6* transgene. Indeed, this misexpression leads to a loss of pigmented cells, similar to that observed with other manipulations (Fig. 4G and H). These observations lend further support to the finding that FGF/MEK/ETS-mediated repression of *Six3/6* in row III of the mid-gastrula neural plate is essential for the specification of row III, including the genesis of lateral pigmented cells in the larval CNS.

A revised fate map for photoreceptor cells

The preceding results show that loss of FGF signaling in row III leads to posterior expansion of *Six3/6* expression, which in turn suppresses correct specification of the lateral a9.49 pigment cell lineage. We sought to determine the consequences of these perturbations on the specification of medial row III cells (a9.33 and a9.37). Previous studies suggest that these lineages form photoreceptor cells of the larval sensory vesicle (Cole and Meinertzhagen, 2004; Horie et al., 2005; Russo et al., 2014). We were surprised to find that inhibition of FGF signaling using *ZicL* > *dnFGFR* did not result in a significant change in the expression of an *Arrestin* reporter gene, which is specifically expressed in photoreceptor cells (Yoshida et al., 2004; Fig. 5A and B). Despite the expansion of *Six3/6* reporter expression, the

Arrestin reporter gene exhibits a discrete expression pattern that does not overlap *Six3/6*. This observation raises the possibility that photoreceptor cells might not arise from medial row III, as has been previously reported.

We further explored this possibility by co-electroporating wild-type embryos with *Dmrt* and *Arrestin* reporter genes. *Dmrt* is specifically expressed in rows III–VI of the mid-gastrula neural plate, and the stable histone fusion protein labels derivatives of these cells at later stages of development (Fig. 1C and D). When we grew these embryos to larval stages, we consistently observed a cluster of *Arrestin*-expressing cells that clearly lack expression of the *Dmrt* reporter (Fig. 5C and C′). Quantitative analysis of *Dmrt* and *Arrestin* reporter colocalization revealed an average Pearson's correlation coefficient of −0.17 ($n = 11$), indicating distinct expression profiles. If photoreceptor cells arose from row III, we would expect to see colocalization of the two reporter genes, since *Dmrt* is expressed in row III, but not more posterior regions of the neural plate. It therefore appears that the *Arrestin*-expressing photoreceptor cells are derived from more posterior regions of the neural plate, most likely medial regions of row II. This origin of the photoreceptor cells is consistent with that determined in another ascidian species, *H. roretzi*, using single-blastomere HRP injection and *Arrestin* in situ hybridization (Taniguchi and Nishida, 2004).

Discussion

The role of FGF signaling in the induction and patterning of the nervous system in both vertebrates and tunicates is well established, but the transcriptional effectors of these signals have not been thoroughly investigated. We have provided evidence that the ETS family transcription factors Ets1/2 and Elk1/3/4 play partially redundant roles in the patterning of both lateral and medial lineages of row III in the anterior neural plate (summarized in Fig. 6). The requirement for Ets1/2 in the lateral a9.49 cells that contribute to pigmented sensory organs within the larval brain has been shown previously (e.g., Squarzoni et al., 2011; Abitua et al., 2012). Our findings suggest that Elk1/3/4, along with Ets1/2, is essential for specification of the medial a9.33 and a9.37 lineages as well. Dominant-negative forms of Ets1/2 and Elk1/3/4 (Ets^{DBD}*:WRPW*; Elk^{DBD}*:WRPW*) lead to ectopic expression of Six3/6, suggesting that these factors are normally required to restrict *Six3/6* expression to row IV, and thereby define the anterior-most neural tube. This repression is essential for specification of row III fates, including pigmented cells. Myt1L is a candidate for such a repressor since it appears to be activated in row III prior to the onset of *Six3/6* expression in row IV. Moreover, Myt1 transcription factors are thought to function as repressors since they have been shown to interact with the Sin3B co-repressor complex (Romm et al., 2005).

It is possible that the differential activities of Ets1/2 and Elk1/3/4 in promoting pigmented cell fates depend on distinct DNA binding activities. Different ETS proteins have been shown to recognize related motifs (GGAA) containing distinct flanking sequences (e.g. Shore et al., 1996; reviewed in Sharrocks (2001)). In addition, ETS factor binding at target enhancers is facilitated by distinct co-factors (Sharrocks, 2001). Our results suggest that co-factors specific to the lateral a9.49 cells of row III are required for activity of Ets1/2 in these cells, whereas different cofactors may facilitate Elk1/3/4 activity in medial a9.33 and a9.37 cells. It has been shown that Nodal signaling is required for medio-lateral patterning of the

Ciona neural plate (Hudson and Yasuo, 2005; Hudson et al., 2007). The lateral cells also receive potential Notch signals, such as Delta-2, and consequently, Nodal and/or Notch signaling might induce localized expression of Ets1/2 cofactors in lateral regions (e.g., the a9.49 lineage). The absence of these cofactors in medial regions might foster Elk1/3/4 activity in the a9.33 and a9.37 lineages.

We also presented evidence that a9.33 and a9.37 do not give rise to photoreceptor neurons, as previously reported. Instead, we suggest that descendants of these cells form ependymal cells and neurons in the larval brain. Some of these ependymal cells may be among the recently described population of "stem-like" cells that differentiate into neurons during metamorphosis (Horie et al., 2011). This speculation is based on the location of the descendants of a9.33 and a9.37 within the sensory vesicle and on the expression of *Myt1L*, which is also expressed in the presumptive ependymal cells of the tail nerve cord (row I), as are *Ets1/2* and *Elk1/3/4* (Fig. 2F′, Supplementary Fig. 3). It is possible that *Myt1L* plays a role in maintaining a "stem-like" state in ependymal cells, or in the specification of distinct neuronal subtypes. *ZicL > Elk^{DBD}:VP64* larvae fail to settle or undergo metamorphosis within 72 hours after fertilization, a period in which control siblings have reached juvenile stages (T.B.G., unpublished observations). Ectopic Elk1/3/4 activity and misexpression of *Myt1L* might result in the loss of neurons involved in settling and/or metamorphosis. *Myt1L* is the putative ortholog of vertebrate MYT1 (myelin transcription factor 1), a zinc finger transcription factor known to regulate genes involved in myelin production in oligodendrocytes (Kim and Hudson, 1992; Armstrong et al., 1995; Kim et al., 1997; Nielsen et al., 2004). While tunicates do not possess myelinated cells, perhaps the tunicate/vertebrate ancestor possessed non-myelinated ependymal cells that expressed an ancestral MYT1-like gene. Changes in the regulatory specificity of MYT1 may have led to expression of myelination genes, and thus emergence of myelinated support cells in jawed vertebrates.

Supplementary Material

Refer to Web version on PubMed Central for supplementary material.

Acknowledgments

We thank members of the Levine lab for helpful discussions. This work was funded by a Grant from the National Institutes of Health (NS 076542) to M.L.

Appendix A. Supporting information

Supplementary data associated with this article can be found in the online version at http://dx.doi.org/10.1016/j.ydbio.2014.12.032.

References

Abitua PB, Wagner E, Navarrete IA, Levine M. Identification of a rudimentary neural crest in a non-vertebrate chordate. Nature. 2012; 492:104–107. [PubMed: 23135395]

Altmann CR, Brivanlou AH. Neural patterning in the vertebrate embryo. Int. Rev. Cytol. 2001; 203:447–482. [PubMed: 11131523]

Armstrong RC, Kim JG, Hudson LD. Expression of myelin transcription factor I (MyTI), a "zinc-finger" DNA-binding protein, in developing oligodendrocytes. Glia. 1995; 14:303–321. [PubMed: 8530187]

Bertrand V, Hudson C, Caillol D, Popovici C, Lemaire P. Neural tissue in ascidian embryos is induced by FGF9/16/20, acting via a combination of maternal GATA and Ets transcription factors. Cell. 2003; 115:615–627. [PubMed: 14651852]

Christiaen L, Jaszczyszyn Y, Kerfant M, Kano S, Thermes V, Joly J-S. Evolutionary modification of mouth position in deuterostomes. Semin. Cell Dev. Biol. 2007; 18:502–511. [PubMed: 17656139]

Christiaen L, Wagner E, Shi W, Levine M. Electroporation of transgenic DNAs in the sea squirt Ciona. Cold Spring Harb. Protoc. 2009a 2009 (pdb.prot5345).

Christiaen L, Wagner E, Shi W, Levine M. Isolation of sea squirt (*Ciona*) gametes, fertilization, dechorionation, and development. Cold Spring Harb. Protoc. 2009b 2009 (pdb.prot5344).

Christiaen L, Wagner E, Shi W, Levine M. Whole-mount in situ hybridization on sea squirt (*Ciona intestinalis*) embryos. Cold Spring Harb. Protoc. 2009c 2009 (pdb.prot5348).

Cole AG, Meinertzhagen IA. The central nervous system of the ascidian larva: mitotic history of cells forming the neural tube in late embryonic *Ciona intestinalis*. Dev. Biol. 2004; 271:239–262. [PubMed: 15223332]

Davidson B, Shi W, Beh J, Christiaen L, Levine M. FGF signaling delineates the cardiac progenitor field in the simple chordate, *Ciona intestinalis*. Genes Dev. 2006; 20:2728–2738. [PubMed: 17015434]

Haupaix N, Abitua PB, Sirour C, Yasuo H, Levine M, Hudson C. Ephrin-mediated restriction of ERK1/2 activity delimits the number of pigment cells in the *Ciona* CNS. Dev. Biol. 2014; 394:170–180. [PubMed: 25062608]

Horie T, Orii H, Nakagawa M. Structure of ocellus photoreceptors in the ascidian *Ciona intestinalis* larva as revealed by an anti-arrestin antibody. J. Neurobiol. 2005; 65:241–250. [PubMed: 16118796]

Horie T, Shinki R, Ogura Y, Kusakabe TG, Satoh N, Sasakura Y. Ependymal cells of chordate larvae are stem-like cells that form the adult nervous system. Nature. 2011; 469:525–528. [PubMed: 21196932]

Hudson C, Lemaire P. Induction of anterior neural fates in the ascidian *Ciona intestinalis*. Mech. Dev. 2001; 100:189–203. [PubMed: 11165477]

Hudson C, Lotito S, Yasuo H. Sequential and combinatorial inputs from Nodal, Delta2/Notch and FGF/MEK/ERK signalling pathways establish a grid-like organisation of distinct cell identities in the ascidian neural plate. Development. 2007; 134:3527–3537. [PubMed: 17728350]

Hudson C, Yasuo H. Patterning across the ascidian neural plate by lateral Nodal signalling sources. Development. 2005; 132:1199–1210. [PubMed: 15750182]

Imai KS, Levine M, Satoh N, Satou Y. Regulatory blueprint for a chordate embryo. Science. 2006; 312:1183–1187. [PubMed: 16728634]

Imai KS, Stolfi A, Levine M, Satou Y. Gene regulatory networks underlying the compartmentalization of the *Ciona* central nervous system. Development. 2009; 136:285–293. [PubMed: 19088089]

Khoueiry P, Rothbacher U, Ohtsuka Y, Daian F, Frangulian E, Roure A, Dubchak I, Lemaire P. A cis-regulatory signature in ascidians and flies, independent of transcription factor binding sites. Curr. Biol. 2010; 20:792–802. [PubMed: 20434338]

Kim JG, Armstrong RC, v Agoston D, Robinsky A, Wiese C, Nagle J, Hudson LD. Myelin transcription factor 1 (Myt1) of the oligodendrocyte lineage, along with a closely related CCHC zinc finger, is expressed in developing neurons in the mammalian central nervous system. J. Neurosci. Res. 1997; 50:272–290. [PubMed: 9373037]

Kim JG, Hudson LD. Novel member of the zinc finger superfamily: a C2-HC finger that recognizes a glia-specific gene. Mol. Cell. Biol. 1992; 12:5632–5639. [PubMed: 1280325]

Lemaire P, Bertrand V, Hudson C. Early steps in the formation of neural tissue in ascidian embryos. Dev. Biol. 2002; 252:151–169. [PubMed: 12482707]

Miya T, Nishida H. An Ets transcription factor, *HrEts*, is target of FGF signaling and involved in induction of notochord, mesenchyme, and brain in ascidian embryos. Dev. Biol. 2003; 261:25–38. [PubMed: 12941619]

Nicol D, Meinertzhagen IA. Cell counts and maps in the larval central nervous system of the ascidian *Ciona intestinalis* (L.). J. Comp. Neurol. 1991; 309:415–429. [PubMed: 1918443]

Nielsen JA, Berndt JA, Hudson LD, Armstrong RC. Myelin transcription factor 1 (Myt1) modulates the proliferation and differentiation of oligodendrocyte lineage cells. Mol. Cell. Neurosci. 2004; 25:111–123. [PubMed: 14962745]

Oikawa T, Yamada T. Molecular biology of the Ets family of transcription factors. Gene. 2003; 303:11–34. [PubMed: 12559563]

Racioppi C, Kamal AK, Razy-Krajka F, Gambardella G, Zanetti L, Bernardo Dd, Sanges R, Christiaen LA, Ristoratore F. Fibroblast growth factor signalling controls nervous system patterning and pigment cell formation in *Ciona intestinalis*. Nat. Commun. 2014; 5:1–17.

Romm E, Nielsen JA, Kim JG, Hudson LD. Myt1 family recruits histone deacetylase to regulate neural transcription. J. Neurochem. 2005; 93:1444–1453. [PubMed: 15935060]

Rothbächer U, Bertrand V, Lamy C, Lemaire P. A combinatorial code of maternal GATA, Ets and beta-catenin-TCF transcription factors specifies and patterns the early ascidian ectoderm. Development. 2007; 134:4023–4032. [PubMed: 17965050]

Russo MT, Racioppi C, Zanetti L, Ristoratore F. Expression of a single prominin homolog in the embryo of the model chordate *Ciona intestinalis*. Gene Expr. Patterns. 2014; 15:38–45. [PubMed: 24755348]

Sanjana NE, Cong L, Zhou Y, Cunniff MM, Feng G, Zhang F. A transcription activator-like effector toolbox for genome engineering. Nat. Protoc. 2012; 7:171–192. [PubMed: 22222791]

Sharrocks AD. The ETS-domain transcription factor family. Nat. Rev. Mol. Cell Biol. 2001; 2:827–837. [PubMed: 11715049]

Sharrocks AD, Brown AL, Ling Y, Yates PR. The ETS-domain transcription factor family. Int. J. Biochem. Cell Biol. 1997; 29:1371–1387. [PubMed: 9570133]

Shi W, Levine M. Ephrin signaling establishes asymmetric cell fates in an endomesoderm lineage of the *Ciona* embryo. Development. 2008; 135:931–940. [PubMed: 18234724]

Shore P, Whitmarsh AJ, Bhaskaran R, Davis RJ, Waltho JP, Sharrocks AD. Determinants of DNA-binding specificity of ETS-domain transcription factors. Mol. Cell. Biol. 1996; 16:3338–3349. [PubMed: 8668149]

Squarzoni P, Parveen F, Zanetti L, Ristoratore F, Spagnuolo A. FGF/MAPK/Ets signaling renders pigment cell precursors competent to respond to Wnt signal by directly controlling *Ci-Tcf* transcription. Development. 2011; 138:1421–1432. [PubMed: 21385767]

Steinmetz PR, Urbach R, Posnien N, Eriksson J, Kostyuchenko RP, Brena C, Guy K, Akam M, Bucher G, Arendt D. *Six3* demarcates the anterior-most developing brain region in bilaterian animals. EvoDevo. 2010; 1:14. [PubMed: 21190549]

Taniguchi K, Nishida H. Tracing cell fate in brain formation during embryogenesis of the ascidian *Halocynthia roretzi*. Dev. Growth Differ. 2004; 46:163–180. [PubMed: 15066195]

Tresser J, Chiba S, Veeman M, El-Nachef D, Newman-Smith E, Horie T, Tsuda M, Smith WC. *doublesex/mab3 related-1* (*dmrt1*) is essential for development of anterior neural plate derivatives in *Ciona*. Development. 2010; 137:2197–2203. [PubMed: 20530547]

Veeman MT, Newman-Smith E, El-Nachef D, Smith WC. The ascidian mouth opening is derived from the anterior neuropore: reassessing the mouth/neural tube relationship in chordate evolution. Dev. Biol. 2010; 344:138–149. [PubMed: 20438724]

Wada H, Saiga H, Satoh N, Holland PW. Tripartite organization of the ancestral chordate brain and the antiquity of placodes: insights from ascidian Pax-2/5/8, Hox and Otx genes. Development. 1998; 125:1113–1122. [PubMed: 9463358]

Wagner E, Levine M. FGF signaling establishes the anterior border of the *Ciona* neural tube. Development. 2012; 139:2351–2359. [PubMed: 22627287]

Yoshida R, Sakurai D, Horie T, Kawakami I, Tsuda M, Kusakabe T. Identification of neuron-specific promoters in *Ciona intestinalis*. Genesis. 2004; 39:130–140. [PubMed: 15170699]

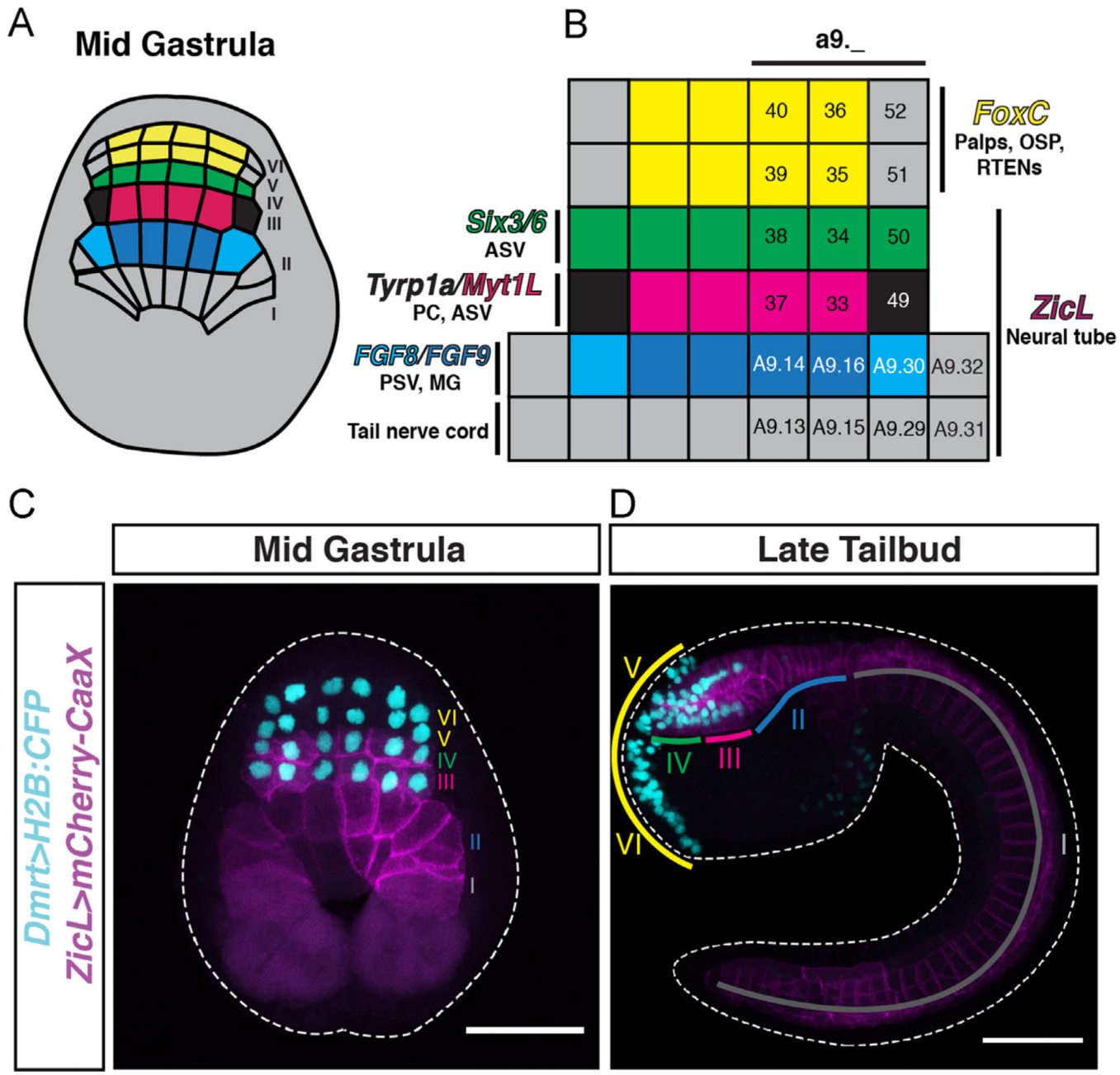

Fig. 1.

The *Ciona* mid-gastrula neural plate. (A) Schematic of a mid-gastrula stage embryo showing the organization of the 6-row neural plate. (B) Gene expression patterns and fates of neural plate territories. Rows V and VI express *FoxC* and give rise to the adhesive palps, oral siphon placode (OSP) and rostral trunk epidermal neurons (RTENs). Row IV expresses *Six3/6* and contributes to the anterior sensory vesicle (ASV). The a9.49 cells in lateral row III express *Tyrp1a* and give rise to pigmented cells (PC). Medial row III cells (a9.33 and a9.37) express *Myt1L* and also contribute to the ASV. The *FGF8*-expressing A9.30 cells in lateral row II form the motor ganglion (MG), whereas medial row II forms posterior sensory vesicle (PSV). Row I contributes to the tail nerve cord. (C, D) Co-electroporation of *Dmrt*

and *ZicL* reporters allows for tracing of cells from the mid-gastrula neural plate (C) to the late tailbud stage (D). Colored lines in (D) indicate territories derived from rows labeled with the corresponding color in (C). Rows V and VI express *Dmrt* exclusively and contribute to the palps, OSP, and peripheral nervous system. *ZicL* and *Dmrt* reporters co-localize in rows III and IV, which give rise to the anterior sensory vesicle. Rows I and II express *ZicL* exclusively and contribute to posterior brain, motor ganglion, and tail nerve cord. Scale bars in (C, D) = 50 μm.

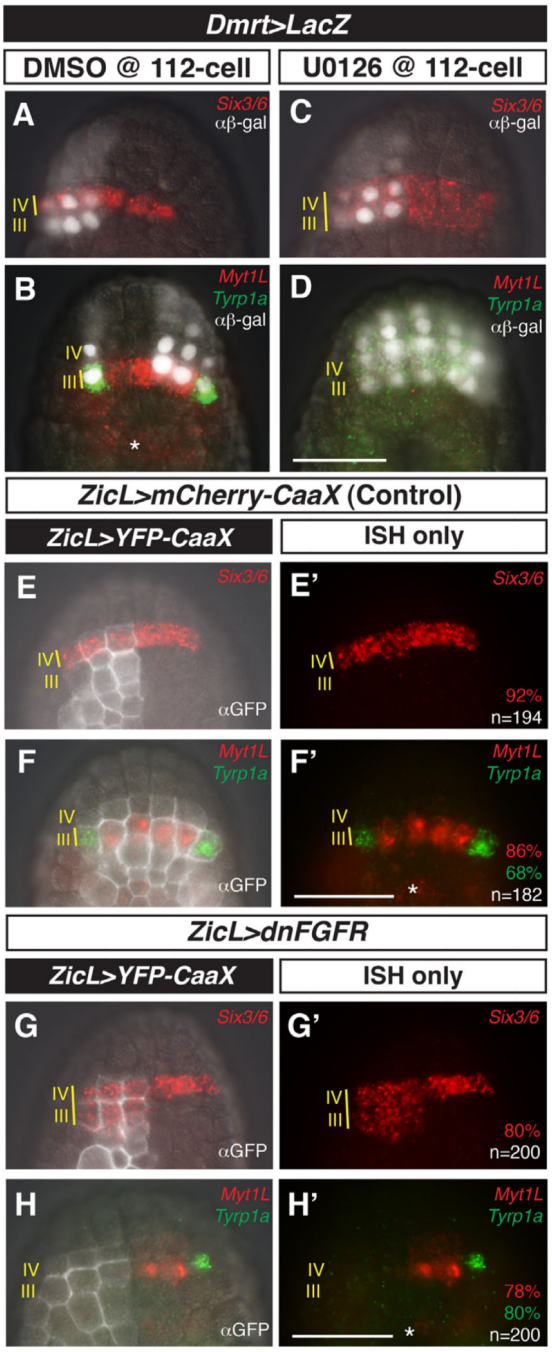

Fig. 2.

MEK/FGF-dependent patterning of rows III and IV of the anterior neural plate. (A–D) Embryos were electroporated with *Dmrt > LacZ* and treated with DMSO (control) or MEK inhibitor U0126 at the 110-cell stage, then fixed at mid-gastrula stage and processed for in situ hybridization with probes against *Six3/6, MyT1L*, and *Tyrp1a* and immunostaining with anti-β-galactosidase antibody (αβ-gal). In control embryos, *Six3/6* expression is restricted to row IV (A). *Myt1L* is expressed in medial row III and *Tyrp1a* is expressed in the lateral a9.49 cells of row III (B). After treatment with U0126, *Six3/6* expression expands

posteriorly into row III (C) at the expense of *Myt1L* and *Tyrp1a* (D). (E–H′) Embryos electroporated with *ZicL* > *YFP-CaaX* alone or co-electroporated with *ZicL* > *dnFGFR*, fixed at mid-gastrula stage, and processed as in (A–D) except using anti-GFP antibody (αGFP). In control embryos, wild-type patterns of *Six3/6, Myt1L*, and *Tyrp1a* expression are observed (E–F′). *ZicL* > *dnFGFR* results in posterior expansion of *Six3/6* and loss of *Myt1L* and *Tyrp1a*, recapitulating U0126 treatment (G–H′). (E–H) ISH overlayed with immunostaining and DIC channels. (E′–H′) ISH channels alone. Embryos in (A, C, E, G, H) are left–right mosaics, owing to unequal inheritance of electroporated plasmids; embryo in (B) also exhibits mosaic inheritance of the *Dmrt* reporter. Scale bars = 50 μm. Asterisks indicate expression of *Myt1L* in row I. See full quantitation of observed phenotypes in Supplementary Fig. 5.

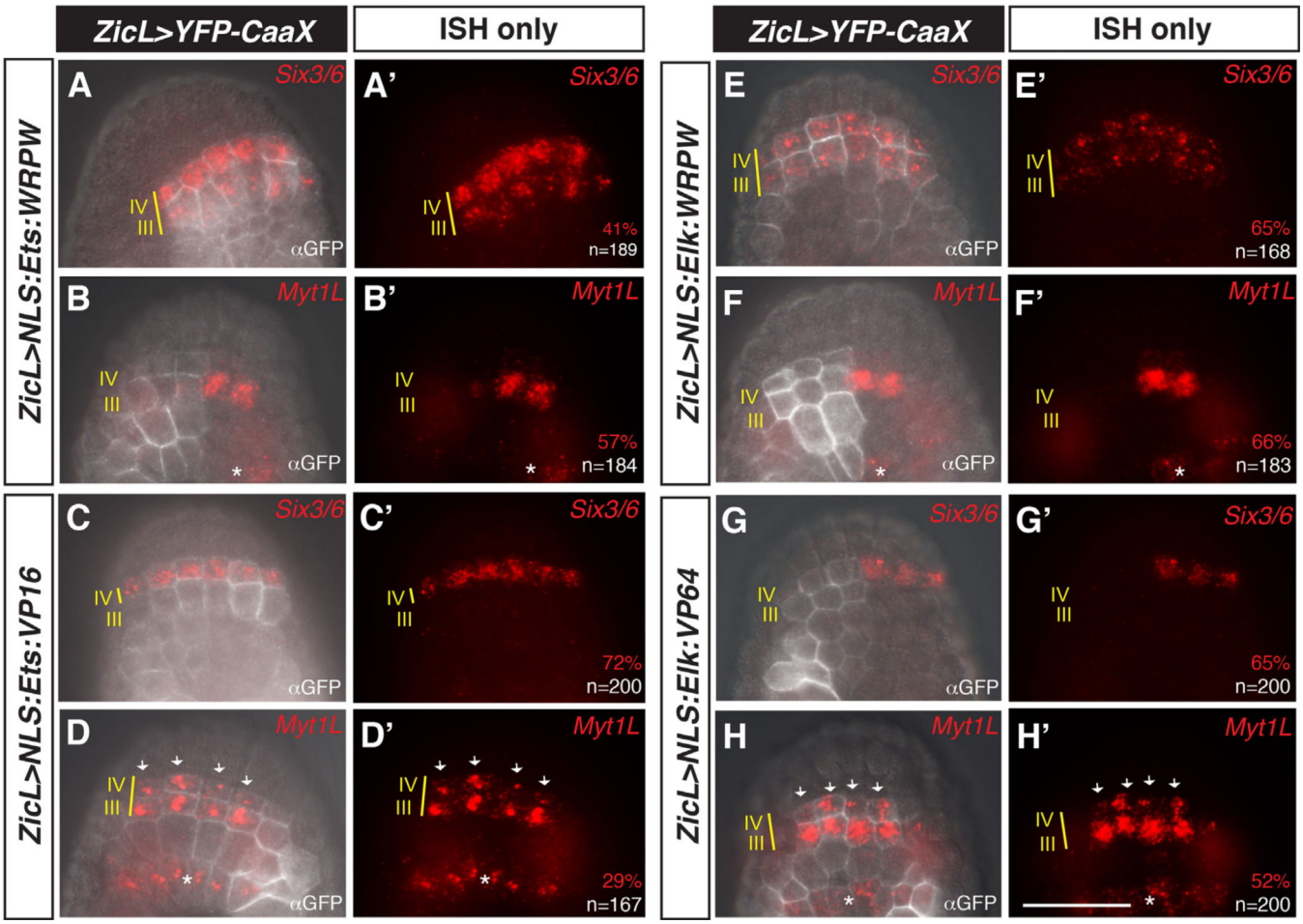

Fig. 3.

Partially redundant roles for Ets1/2 and Elk1/3/4 in the anterior neural plate. (A–D′) Embryos were co-electroporated with *ZicL* > *YFP-CaaX* and *ZicL* > *Ets:WRPW* (A–B′) or *ZicL* > *Ets:VP16* (C–D′), and then assayed for expression of *Six3/6* (A, A′, C, C′), or *Myt1L* (B, B′, D, D′) at mid-gastrula stage by in situ hybridization and immunohistochemistry with GFP antibody (αGFP). *ZicL* > *Ets:WRPW* leads to modest expansion of *Six3/6* (A, A′) and loss of *Myt1L* (B, B′). *ZicL* > *Ets:VP16* embryos show mostly wild-type expression of *Six3/6* (C, C′) and a moderate expansion of *Myt1L* (arrows in D, D′). (E–H′) Similar to (A–D′), except embryos were electroporated with *ZicL* > *Elk:WRPW* (E–F′) or *ZicL* > *Elk:VP64* (G–H′). *ZicL* > *Elk:WRPW* has a slightly stronger effect on *Six3/6* expansion into row III (E, E′). This expansion occurs at the expense of *Myt1L* (F, F′). *ZicL* > *Elk:VP64* results in repression of *Six3/6* in row IV (G, G′) and expansion of *Myt1L* expression (arrows in H, H′). Embryos in (B, B′), (F, F′) and (G, G′) are left–right mosaics, owing to unequal inheritance of electroporated plasmids. Scale bar = 50 μm. Asterisks indicate expression of *Myt1L* in row I. See full quantitation of observed phenotypes in Supplementary Fig. 5.

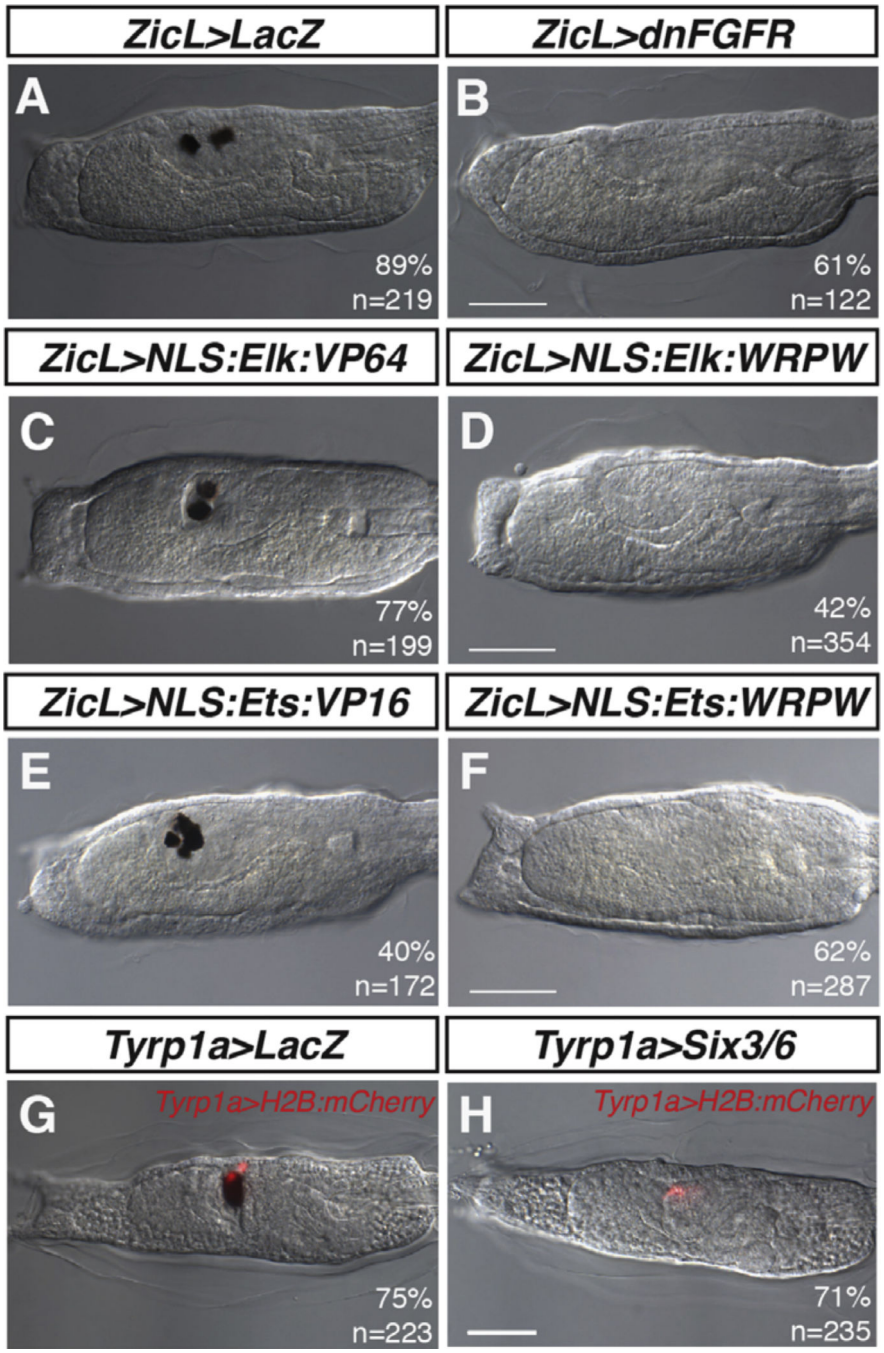

Fig. 4.

Ets1/2 and Elk1/3/4 have distinct larval phenotypes. (A–B) Control and FGF-inhibited larvae. (A) Control larvae possess two pigmented cells within the sensory vesicle. (B) *ZicL > dnFGFR* results in complete loss of pigmented cells in the majority of larvae. (C–D) Misexpression of Elk1/3/4 fusion proteins. (C) *ZicL > Elk:VP64* larvae contain 2 pigmented cells, comparable to controls. (D) *ZicL > Elk:WRPW* results in fewer pigmented cells relative to controls, similar to *ZicL > dnFGFR*. (E, F) Misexpression of Ets fusion proteins. (E) *ZicL > Ets:VP16* is sufficient to produce supernumerary pigmented cells, whereas *ZicL*

> *Ets:WRPW* results in loss of pigmentation (F), as previously described. (G, H) Larvae electroporated with *Tyrp1a* > *LacZ* (G) or *Tyrp1a* > *Six3/6* (H). Misexpression of *Six3/6* in the pigmented cell lineage is sufficient to abolish pigmentation. Scale bars = 50 μm.

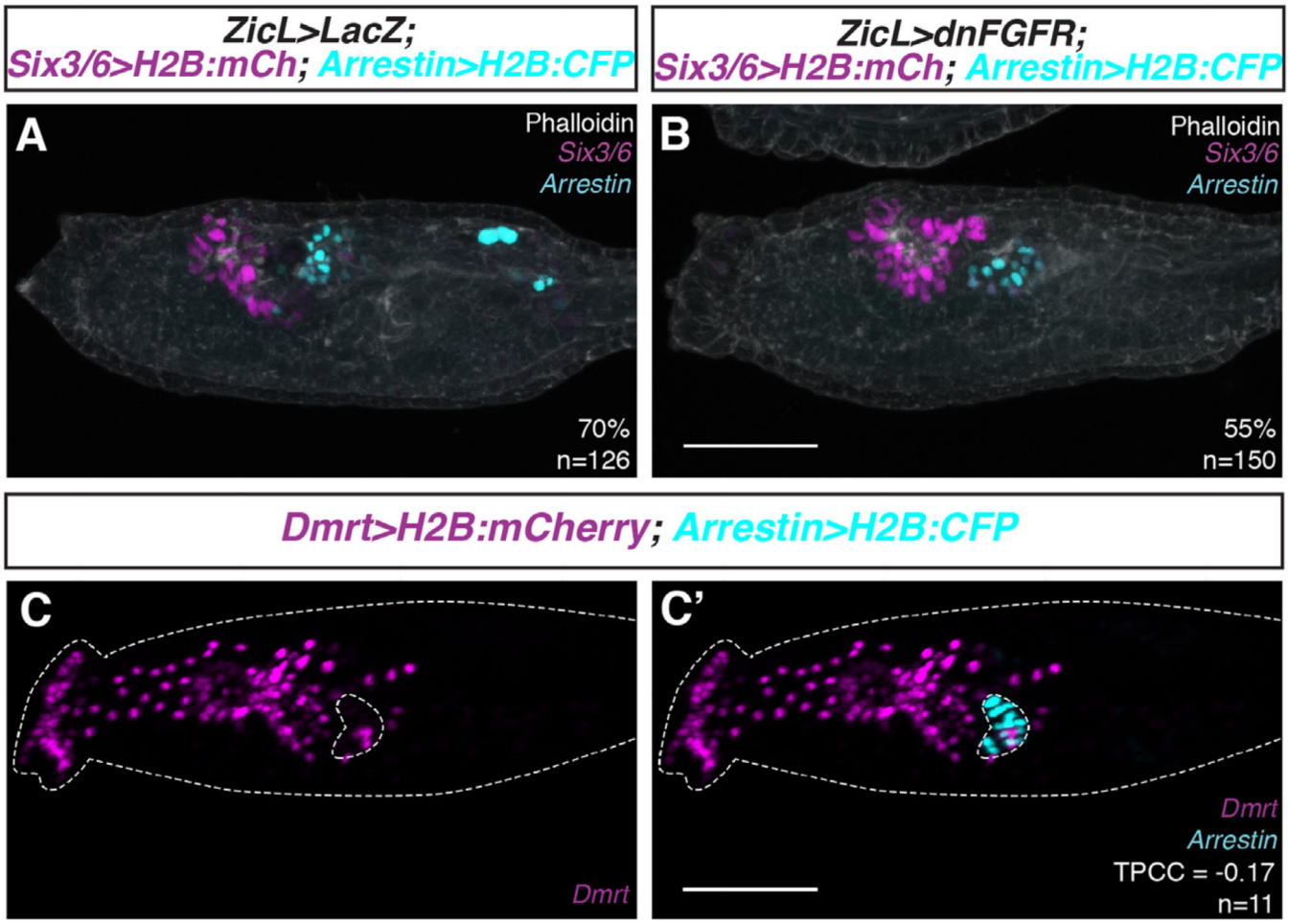

Fig. 5.

A revised origin of *Ciona* photoreceptor cells. (A, B) Control and *ZicL* > *dnFGFR* embryos were co-electroporated with reporters for *Six3/6* and *Arrestin*, and then grown to larval stage. (A) *Arrestin* reporter labels a cluster of cells surrounding the ocellus, posterior to the *Six3/6* expression domain. (B) Inhibition of FGF signaling results in posterior expansion of the *Six3/6* reporter, but no significant change in *Arrestin* reporter expression. *Arrestin* reporter does not colocalize with ectopic *Six3/6* reporter. (C, C′) Embryos were co-electroporated with reporters for *Dmrt* and *Arrestin* and grown to larval stage. Clusters of *Arrestin*+ cells are consistently observed posterior to the *Dmrt* expression domain. Scale bars = 50 μm.

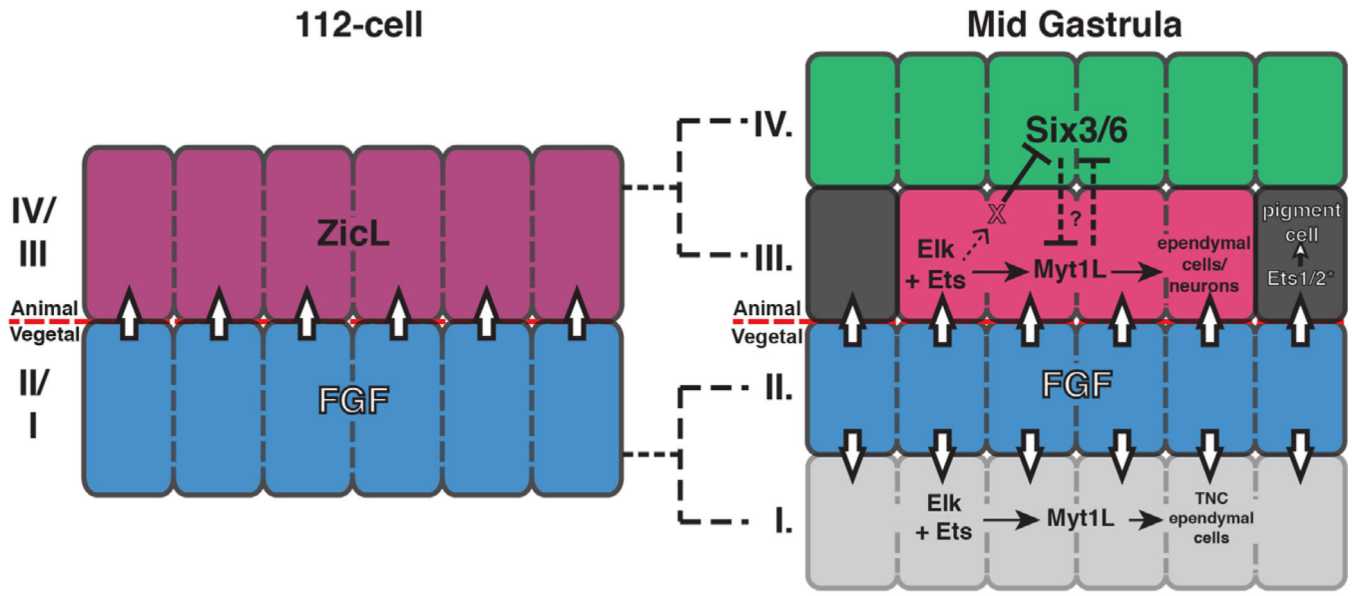

Fig. 6.

Summary of FGF-dependent patterning in the mid-gastrula neural plate. FGF signaling at the 112-cell stages leads to asymmetric division of the row III/row IV precursors. Activated Ets1/2 and Elk1/3/4 lead indirectly to repression of *Six3/6* in row III and expression of *Myt1L* in row I and medial row III. These *Myt1L*+ cells contribute to ependymal cells of the tail nerve cord (TNC) and sensory vesicle (SV). Ets/Pnt2 mediates expression of *Tyrp1a* and ultimately promotes pigment cell formation in the lateral a9.49 lineage of row III.